

# Depletion of hCINAP by RNA interference causes defects in Cajal body formation, histone transcription, and cell viability

Jinfang Zhang · Feiyun Zhang · Xiaofeng Zheng

Received: 15 October 2009 / Revised: 25 January 2010 / Accepted: 2 February 2010 / Published online: 26 February 2010  
© Springer Basel AG 2010

**Abstract** hCINAP is a highly conserved and ubiquitously expressed protein in eukaryotic organisms and its overexpression decreases the average number of Cajal bodies (CBs) with diverse nuclear functions. Here, we report that hCINAP is associated with important components of CBs. Depletion of hCINAP by RNA interference causes defects in CB formation and disrupts subcellular localizations of its components including coilin, survival motor neurons protein, spliceosomal small nuclear ribonucleoproteins, and nuclear protein ataxia-telangiectasia. Moreover, knock-down of hCINAP expression results in marked reduction of histone transcription, lower levels of U small nuclear RNAs (U1, U2, U4, and U5), and a loss of cell viability. Detection of increased caspase-3 activities in hCINAP-depleted cells indicate that apoptosis is one of the reasons for the loss of viability. Altogether, these data suggest that hCINAP is essential for the formation of canonical CBs, histone transcription, and cell viability.

**Keywords** Cajal body · hCINAP · RNAi · Histone transcription · Cell viability

## Abbreviations

hCINAP	Human coilin interacting nuclear ATPase protein
CBs	Cajal bodies
RNAi	RNA interference
SMN	Survival motor neurons
snRNAs	Small nuclear RNAs
snRNPs	Small nuclear ribonucleoproteins
NPAT	Nuclear protein ataxia-telangiectasia
ADLP	Adrenal gland protein AD-004-like protein

## Introduction

Cajal bodies (CBs) are multifunctional and dynamic sub-nuclear organelles present in mammalian, amphibian, insect, plant, and yeast cells [1, 2]. So far, the spliceosomal U small nuclear ribonucleoproteins (snRNPs), the U7 snRNP involved in histone mRNA 3'-end processing, the U3 and many other small nucleolar RNPs (snoRNPs) that are involved in pre-rRNA processing, the small Cajal body RNPs (scaRNPs) that are involved in nucleotide modification of spliceosomal small nuclear RNAs (snRNAs), human telomerase RNP [3, 4], and many transcriptional factors including histone and snRNAs transcriptional factors, have been shown to be localized in CBs [2, 5–12]. It is also believed that CBs are involved in regulating histone and snRNAs genes transcription and final maturation of snRNPs and snoRNPs [2, 13, 14].

Coilin is highly enriched in CBs and has been widely used as a molecular marker for CBs in mammalian cells [15]. It has been shown by Mettera and colleagues that coilin is essential for proper formation and/or maintenance of CBs, and the loss of coilin's C-terminus results in a

---

J. Zhang · X. Zheng  
National Laboratory of Protein Engineering and Plant Genetic Engineering, Peking University, Beijing 100871, China

J. Zhang · X. Zheng (✉)  
Department of Biochemistry and Molecular Biology,  
College of Life Sciences, Peking University,  
Beijing 100871, China  
e-mail: xiaofengz@pku.edu.cn

F. Zhang  
Department of Biochemistry and Molecular Biology,  
College of Life Sciences, Capital Normal University,  
Beijing 100037, China

failure of recruitment of the survival motor neurons (SMN) protein and the Sm snRNPs to residual CBs [16]. Recent studies have proved that the C-terminal domain of coilin interacts with SMN [17] and Sm [18]. Furthermore, the number of CBs is also mediated by the C-terminus of coilin [19]. These data suggest that C-terminus of coilin is involved either in the targeting or in the retention of SMN and snRNP complexes in CBs and is essential for normal formation of CBs.

In addition to coilin, SMN is also a marker protein for CBs. Deletion or mutation in the SMN gene results in the spinal muscular atrophy (SMA) disease [20, 21]. The SMN protein is present in both the cytoplasm and the nucleus where it localizes to CBs. In the cytoplasm, SMN is part of a macromolecular complex that mediates the assembly of spliceosomal U snRNPs [22]. The assembled snRNPs, presumably associated with SMN, enter the nucleus and target to CBs, where the U snRNAs undergo further modification of 2'-O-methylation and pseudouridylation [23]. Some recent studies have shown that depletion of SMN by RNAi induces defects in the formation of CBs [24–26].

CBs have also been shown to interact with histone gene clusters and have been implicated in regulating histone gene transcription [27]. The CB component NPAT is required for activation of multiple histone genes and S-phase entry mainly through its phosphorylation or recruiting other transcription factors to histone gene promoters [28, 29]. NPAT-containing CBs appear to preferentially co-localize with histone loci, and their number is increased in the late G1 and S-phase [30]. Cells lacking NPAT lead to cell cycle arrest prior to S-phase entry, and this arrest occurs concurrently with dissociation of the coilin from CBs, suggesting a role for NPAT in maintaining proper CB assembly.

hCINAP, also named hAK6 [31, 32], is a ubiquitously expressed protein. The sequence of hCINAP is highly conserved from human to *C. elegans*, *Drosophila*, *Arabidopsis*, and yeast [31, 33]. It has been proved that hCINAP interacts with coilin through the C-terminal residues of coilin, which controls the number of CBs, and that over-expression of hCINAP in HeLa cells leads to a decrease of the average number of CBs per nucleus [32]. These results suggest that hCINAP probably plays an important role in regulating the formation of canonical CBs.

In this study, we identified hCINAP as an essential constituent of CB by immunoprecipitation and immunofluorescent analyses, and demonstrated that depletion of hCINAP causes defects in the formation of canonical CBs and disrupts the subcellular localization of the essential components of CBs including coilin, SMN, spliceosomal snRNP, fibrillarin, and NPAT. We also found that hCINAP depletion results in reduction of histone transcription and cell viability.

## Materials and methods

### Cell culture and preparation of nuclear extracts

HeLa or HEK 293T cells were grown in IMDM medium (Gibco) containing 10% fetal calf serum (Hyclone) at 37°C in 5% CO<sub>2</sub>. Twelve 200-mL bottles of cells with 90–95% confluent were harvested by scraping the cells into phosphate-buffered saline (PBS), packed by centrifuge at 720g for 10 min. Cells were then washed twice with ice-cold PBS and resuspended in ten times the packed cell volumes (PCV) of hypotonic buffer (10 mM Tris-HCl, pH 7.9, 10 mM NaCl, 1.5 mM MgCl<sub>2</sub>, 0.5 mM PMSF, 1 µg/mL leupeptin, 1 µg/mL aprotinin, and 1 µg/mL pepstatin) on ice for 15 min, and lysed by 15 strokes of Dounce homogenizer (B type pestle) from KONTES. The homogenate centrifuged at 720g for 10 min to pellet nuclei. The supernatant was decanted carefully and the pellet was washed once using hypotonic buffer. These nuclei were resuspended in 4 mL of cell lysis buffer (50 mM Tris, pH 8.0, 150 mM NaCl, 0.5% NP-40, 1 mM EDTA, 1 mM PMSF, 1 µg/mL leupeptin, 1 µg/mL aprotinin, and 1 µg/mL pepstatin), sonicated at 100 W for three cycles of 3 s each, and centrifuged at 23,500g for 15 min. The supernatants were designated as the nuclear extracts.

### Immunoprecipitation from nuclear extracts of HeLa cells and Western blot analysis

Rabbit polyclonal anti-hCINAP was prepared by immunizing a rabbit and purified using an affinity column containing the immobilized hCINAP. Nuclear extracts were incubated with anti-hCINAP, anti-coilin, or control preimmune IgG at 4°C overnight. Then, protein G Sepharose was added and incubated for 4 h. The Sepharose beads were washed three times with lysis buffer. The precipitated proteins were fractionated on 15% SDS-PAGE and transferred to nitrocellulose membrane (GE Healthcare). The membrane was blocked with 5% milk, followed by incubation with anti-hCINAP (1:1,000), anti-coilin, anti-SMN, anti-fibrillarin, anti-NPAT, or anti-SC35 (1:500) primary antibodies, and then horseradish peroxidase (HRP)-conjugated goat anti-rabbit IgG or anti-mouse IgG (1:5,000) secondary antibody. Finally, the blots were incubated with ECL chemiluminescence reagent (Pierce Biotechnology) and exposed to X-ray film (Kodak).

### RNA interference and transfection

Three specific small interfering RNA (siRNA) duplexes targeting the hCINAP gene (accession no. AJ878881) were designed and synthesized as 21mers with 3'-dTdT overhangs as follows: siRNA1, 5'-CAGAGUAGUUGAUGAGUUA;

siRNA2, 5'-GAGAGAAGGUGGAGUUAUU; siRNA3, 5'-UGGCUAUGAUGAAGAGUAU. The scrambled oligonucleotide sequence, 5'-UUCUCCGAACGUGUCACGU, was used as a negative control.

Cells were transfected with the synthesized hCINAP-specific siRNA or control siRNA duplex using Lipofectamin<sup>TM</sup> 2000 (Invitrogen) according to the manufacturer's protocol. Briefly, about  $2 \times 10^5$  cells were seeded in 2 mL of growth medium 1 day before transfection. When the confluence reached 70–80%, 40 nM of each synthesized siRNA was transfected into the cells. Preliminary time course analysis showed that the most significant reduction in the hCINAP protein expression was observed at 72 h after transfection with siRNA1. Therefore, this time point was used for subsequent experiments.

pSUPER RNAi system is a vector system for expression of small interfering RNAs (siRNAs) and can cause more efficient and specific down-regulation of gene expression in mammalian cells [34]. To generate stable loss-of-function phenotypes efficiently, annealed oligonucleotides (siRNA1) of hCINAP were cloned into the *Bgl*III/*Hind*III sites of pSUPER followed the manufacturer's protocol (Oligoengine). HeLa cells were transfected with 4  $\mu$ g pSUPER-siRNA1 or control pSUPER vector for 24 h and then selected with 1  $\mu$ g/mL puromycin for 48 h prior to assay.

#### RNA isolation and RT-PCR

Total RNAs were extracted from the cells treated either with hCINAP-specific siRNA or control siRNA using TRIZOL Reagent (Invitrogen), and the cDNAs were amplified by reverse transcriptase coupled PCR (RT-PCR) (AccessQuick<sup>TM</sup> RT-PCR System; Promega) following the manufacturer's instructions. The expression level of the hCINAP gene in hCINAP-depleted cells was compared with that of control cells. To minimize mRNA quantification errors and to correct for sample-loading variations,  $\beta$ -actin gene was used as an internal control, and the relative expression ratio was based on the expression of a target gene relative to that of  $\beta$ -actin. Primers used for detecting hCINAP transcripts were 5'-GGTGGAGTTATTGTTGATTAC and 5'-CCTTGTAGGATGCTGTGGC.

#### Immunofluorescence analysis

HeLa cells were cultured for 72 h on glass coverslips after transfection with siRNA duplexes. Cells were fixed with 3.7% paraformaldehyde in PBS for 20 min at room temperature and permeabilized with 0.3% (v/v) TritonX-100 in PBS for 10 min on ice, and then blocked with 3% bovine serum albumin in PBS with 0.5% Tween-20 for 20 min at room temperature. Cells were incubated with primary antibodies overnight at 4°C, washed, and incubated with

specific fluorescently labeled secondary antibodies for 1 h at 37°C. The following antibodies were used: rabbit polyclonal anti-hCINAP was prepared as described above; mouse monoclonal anti-coilin, mouse monoclonal anti-SMN, mouse monoclonal anti-2,2,7-trimethylguanosine, and rabbit polyclonal anti-fibrillarin were purchased from Santa Cruz Biotechnology; mouse monoclonal anti-NPAT was from BD Transduction Laboratories; and Rhodamine (TRITC)-conjugated goat anti-rabbit IgG and Fluorescein (FITC)-conjugated goat anti-mouse IgG were from Zhongshan Golden Bridge Biotechnology.

Fluorescence microscopy was performed by using a confocal laser scanning microscope (Leica TCS SP5). All the images were captured and processed under identical conditions by keeping all microscope parameters constant, including scan speed, excitation and emission wavelengths using Leica confocal software.

#### Co-immunoprecipitation

To examine the interaction between the hCINAP and NPAT, co-immunoprecipitation was carried out according to procedures described previously [35]. Briefly, HEK 293T cells were cotransfected with pRK-Flag-hCINAP and pCMV-NPAT (a kind gift from Dr. Jiyong Zhao at University of Rochester Medical Center). After 48 h, cells were collected and lysed. The supernatant was incubated with anti-Flag or anti-NPAT monoclonal antibodies or control IgG. Nuclear extracts were also incubated with anti-hCINAP or control preimmune IgG at 4°C overnight. Then, protein G Sepharose was added and incubated for 4 h. The Sepharose beads were washed three times with lysis buffer. The precipitated proteins were fractionated on 15% SDS-PAGE and transferred to nitrocellulose membrane (GE Healthcare). Membranes were probed with primary and secondary antibodies.

#### U snRNAs and histone mRNA evaluation

HeLa cells transfected with pSUPER-hCINAP (siRNA1) or control pSUPER vector for 24 h were selected with 1  $\mu$ g/mL puromycin for 48 h. The total RNAs were extracted and RT-PCR was performed to evaluate the U snRNAs and histone mRNA levels [36] with the following primers:

- U1, forward: 5'-gataccatgatcacgaaggtggtt, reverse: 5'-ca caaattatgcagtcgagttcc;
- U2, forward: 5'-tttgctaagatcaagtgtagtctgttc, reverse: 5'-aatccattaatatattgtctcggataga;
- U4, forward: 5'-gcgcgattattgctaattgaaa, reverse: 5'-aaaaa ttgccagtccgacta;
- U5, forward: 5'-ggtttctcttcagatgcataaatc, reverse: 5'-ctc aaaaaattgggtaagactcaga;

U6, forward: 5'-gcttcggcagcacatatactaaat; reverse: 5'-acgaatttcgctgcctcctt;  
 H2A, forward: 5'-atgtctggacgtggcaagca, reverse: 5'-agcttggtgagctcctcgtc;  
 H2B, forward: 5'-ccgaagaaggctccaagaa, reverse: 5'-ttattggagctggtgtacttg;  
 H3, forward: 5'-agctcgcaagtctaccggcg, reverse: 5'-cgtttagcgtgaatagcgca;  
 H4, forward: 5'-caaagtctgcgcgacaaca, reverse: 5'-gccgcgcaaagccatacagg.

### Flow cytometry

HeLa cells were transfected with control or hCINAP siRNAs for 72 h. Cells were then harvested, washed in PBS, resuspended in ice-cold 70% ethanol, and fixed for at least 30 min. The cells were collected by centrifugation and stained in a solution containing 1% FBS, 50  $\mu$ g/mL propidium iodide and 100  $\mu$ g/mL RNase A in PBS for 30 min. Flow cytometry was performed on a FACSCalibur cytometer and data were analyzed using the CellQuest Pro software (BD Biosciences).

### Cell viability assay

For the assay,  $5 \times 10^3$  cells were seeded per well in 96-well plates in 100  $\mu$ L of growth medium in the absence of antibiotics. Then, 24 h later, 2 nM hCINAP-specific siRNA or control siRNA was transfected into cells using Lipofectamine<sup>TM</sup> 2000. Next, 20  $\mu$ L of CellTiter 96<sup>R</sup> AQueous One Solution Reagent (Promega) was pipetted into each well 72 h after transfection. The plate was incubated at 37°C for 2 h. Then, the absorbance at 490 nm was measured using an ELISA plate reader (DNM-9602; Prolong). The number of cells was calculated using the standard curve. The result was expressed as mean  $\pm$  SD of five independent experiments. The significance was determined using Student's *t* distribution.

### Caspase-3 activity assay

The activity of caspase-3 was measured by using the CaspACE<sup>TM</sup> assay system, according to the manufacturer's protocol (Promega). Briefly, HEK 293T cells were transfected with hCINAP RNAi plasmid (pSUPER-siRNA1) and pSUPER-empty vector, respectively. Then, 72 h after transfection, cells were collected and lysed. The concentration of total protein was determined by the Bio-Rad protein assay and 40  $\mu$ g protein of each extract was used to detect the caspase-3 activity. After adding caspase-3 substrate Ac-DEVD-*p*-nitroaniline (pNA), the 96-well plates were covered and incubated at 37°C for 3 h. The pNA

released from the substrate, upon cleavage with caspase-3, was monitored by a spectrophotometer at a wave length of 405 nm (DNM-9602; Prolong). Caspase-3 activity was calculated by pNA calibration curves and was expressed as nM pNA/min per mg protein.

## Results

### hCINAP is associated with components of CBs

It has been reported that hCINAP interacts with coilin by the carboxyl-terminal 214 amino acid residues of coilin and that overexpression of hCINAP leads to a decrease in the average number of CBs per nucleus [32]. Coilin, which can interact with many components of CB, is a marker protein of CB [2]. These results prompted us to test whether hCINAP is an element of CB.

We firstly verified the specificity of the polyclonal anti-hCINAP generated from rabbit by western blot analysis. As shown in Fig. 1a, both endogenous and recombinant hCINAP were recognized specifically. Therefore, anti-hCINAP was used to perform immunoprecipitation assay using the nuclear extract of HEK 293T cells. Proteins that immunoprecipitated with anti-hCINAP were subjected to western blot analyses with various antibodies (Fig. 1b). The components of CBs, coilin, SMN, fibrillarin, and NPAT were detected in anti-hCINAP immunoprecipitates (Fig. 1b, left panel). Reciprocally, western blot analysis of anti-coilin immunoprecipitates demonstrated that hCINAP, SMN, fibrillarin, and NPAT also co-existed in a complex with coilin (Fig. 1b, right panel). Moreover, a control experiment using rabbit preimmune IgG did not precipitate any protein, and an irrelevant nuclear protein, SC35, was

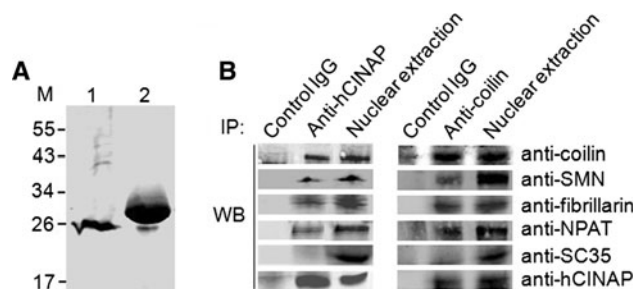


**Fig. 1** hCINAP is associated with major components of CBs. **a** The specificity of hCINAP antibody was confirmed by western blot analysis. Lane 1, endogenous expressed hCINAP in HEK 293 T cells; lane 2, purified recombinant His-tagged hCINAP from *E. coli* (BL21DE3). **b** hCINAP is associated with major components of CBs. The nuclear extraction of HEK 293 T cells were precipitated by polyclonal anti-hCINAP (left panel) and by anti-coilin (right panel), respectively, and analyzed by western blotting using the different antibodies indicated

undetectable in both the anti-hCINAP and anti-coilin immunoprecipitates. In addition, indirect immunofluorescence analysis by confocal laser microscopy confirmed that hCINAP co-localized with coilin (see Fig. 3a, below: white arrows, upper panel) and NPAT (see Fig. 5a, below: white arrows, upper panel) in CBs, respectively. These results demonstrated that hCINAP is a component of CBs.

### Knockdown of hCINAP expression by RNAi

To further investigate the function of the hCINAP protein in CBs, we depleted its expression level in HeLa or HEK 293T cells by RNAi. Three hCINAP-specific siRNAs and a control siRNA were designed, synthesized, and transfected into HeLa cells. The efficient reduction of hCINAP expression was verified by RT-PCR and western blot analyses. Compared with control siRNA, the mRNA levels of hCINAP were reduced to 18.3, 29.3, and 35.7% of the control for siRNA1, siRNA2, and siRNA3, respectively, 72 h after transfection (Fig. 2a). Consistent with this observation, the expression of hCINAP protein was decreased remarkably (Fig. 2b). Similar results were obtained in a HEK 293T cell line (data not shown). Therefore, hCINAP-specific siRNA1 was chosen to treat the cells for 72 h in the following experiments. In the cells that transiently transfected with synthesized hCINAP-siRNAs, the hCINAP-mRNA level could be reduced to ~20% of

control (Fig. 2a), and a similar decrease in hCINAP protein expression was observed (Fig. 2b), whereas in the cells that transfected with pSUPER-hCINAP (siRNA1) followed puromycin selection, the mRNA level of hCINAP could be further reduced to ~5% of control (Fig. 2c), and the expression of hCINAP protein was hardly detected by western blotting (Fig. 2d).

### Depletion of hCINAP results in defects in the formation of canonical CBs

Recent studies have shown that depletion of the components of CBs, SMN [24–26], ZPR1 [37], and FLASH [38] by RNAi leads to loss of canonical CBs. Therefore, we were interested in investigating whether depletion of hCINAP could affect the formation of CBs.

The homeostasis of CBs was determined in hCINAP-depleted cells by immunofluorescence experiments employing an antibody against coilin. In control cells, hCINAP and coilin were observed to co-localize in canonical CBs (Fig. 3a, white arrows, upper panels). While in hCINAP-depleted cells, coilin was distributed in numerous smaller and irregular foci throughout the entire nucleus (Fig. 3a, lower panels). Basic statistics showed that canonical CBs disappeared in 88% of cells depleted of hCINAP. These results suggest that depletion of hCINAP results in defects in the formation of canonical CBs.

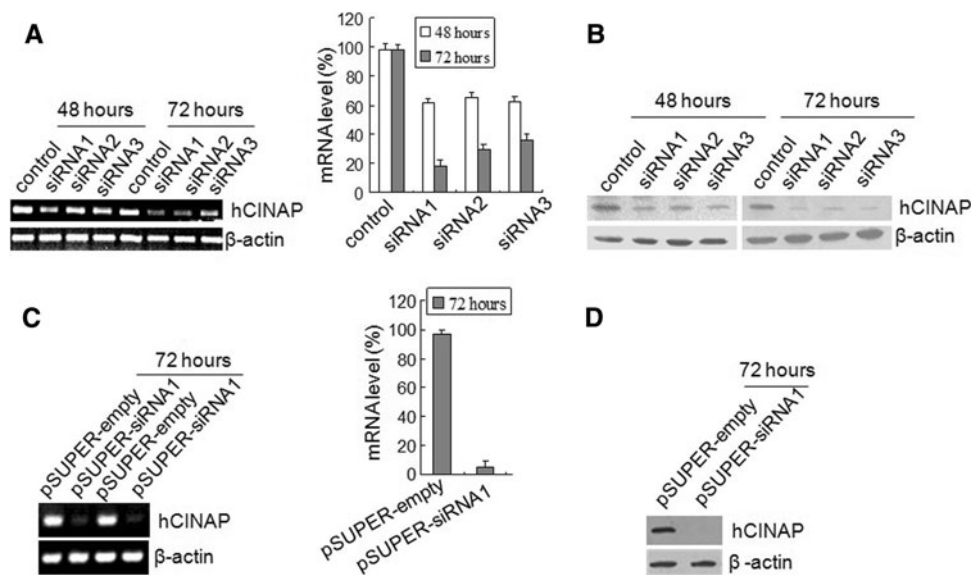


**Fig. 2** Knockdown of hCINAP expression in HeLa cells by RNAi. **a** Specific reduction of hCINAP mRNA expression. HeLa cells were transfected with a synthesized control non-silencing siRNA or three hCINAP-specific siRNAs for 48 h or 72 h, total RNAs were isolated, and RT-PCR analysis was performed (*left panel*). Quantification of hCINAP mRNA was performed using AlphaImager™ software (*right panel*). The relative amounts (mean  $\pm$  SD,  $n = 3$ ) of hCINAP mRNA normalized to  $\beta$ -actin are presented as a *bar graph*. **b** Western blot

analysis on depletion of hCINAP in RNAi treated cells.  $\beta$ -actin protein was used as the loading equal amounts of total protein in each lane. **c** RT-PCR analysis on depletion of hCINAP in pSUPER-hCINAP (siRNA1) transfected cells (*left panel*). Quantification of hCINAP mRNA was performed using AlphaImager™ software (*right panel*). **d** Western blotting analysis on depletion of hCINAP in pSUPER-hCINAP (siRNA1) treated-cells.  $\beta$ -actin protein was used as the loading equal amounts of total protein in each lane

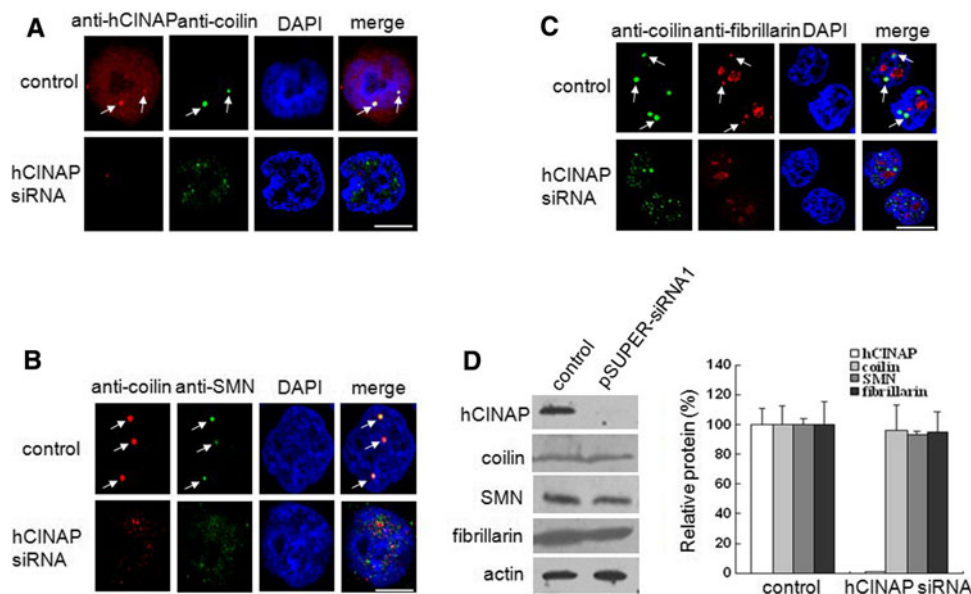


**Fig. 3** Depletion of hCINAP results in defective formation of CBs and disrupts the normal localization of coilin, SMN, and fibrillarin in CBs. HeLa cells were transfected with a control or hCINAP-specific siRNA and stained with antibodies indicated. **a** Re-localization of coilin in hCINAP-depleted cells. The subcellular localization of hCINAP (red) and coilin (green) was examined by immunofluorescence analysis. **b** Depletion of hCINAP disrupts the normal localization of SMN in nucleus. Cells were stained with antibodies against SMN (green) and coilin (red). **c** hCINAP deficiency causes defects in fibrillarin localization in CBs. HeLa cells transfected with a

control or hCINAP-specific siRNA were stained with antibodies to coilin (green) and fibrillarin (red). **d** hCINAP deficiency does not affect the protein expression levels of coilin, SMN, or fibrillarin. The expression of coilin, SMN, and fibrillarin in HeLa cells transfected with pSUPER-hCINAP (siRNA1) was examined by western blot analysis (left panel). Quantitation of immunoblots was performed using AlphaMager™ software (right panel). The relative amounts (mean  $\pm$  SD,  $n = 3$ ) of proteins normalized to  $\beta$ -actin are presented as a bar graph. In **a–c**, CBs are indicated with a white arrow and the nucleus was stained with DAPI (blue). Scale bar 10  $\mu$ m

#### Depletion of hCINAP disrupts the normal localization of SMN in nucleus

The SMN protein, which interacts with coilin, is an essential component for CBs. Depletion of SMN in HeLa cells by RNAi has been shown to induce defects in the formation of CBs [24, 25]. Detection of SMN protein in hCINAP immunoprecipitates (Fig. 1b) drove us to examine the effect of hCINAP depletion on the localization of SMN. Confocal immunofluorescence microscopy analysis showed that in control cells, SMN co-localized with coilin in CBs (Fig. 3b, white arrows, upper panels). In contrast, in hCINAP-depleted cells, the canonical CBs disappeared (Fig. 3b, lower panels). Moreover, a redistribution of SMN into numerous small foci occurred upon hCINAP depletion (Fig. 3b, lower panels). These results suggest that is essential for the formation of canonical CBs and the normal localization of SMN in nucleus.

#### hCINAP deficiency alters the localization patterns of fibrillarin in extra-nucleolar foci

CBs also play an important role in the maturation of snoRNPs [13, 39]. Based on the conserved RNA signature-sequence elements and characteristic secondary structures, snoRNPs are classified into two families, C/D box and

H/ACA box [39]. The methyltransferase fibrillarin, which is used as a marker for nucleoli, is a core component of mature C/D box snoRNP and co-localizes with coilin in CBs. In order to understand whether depletion of hCINAP can influence the normal location of fibrillarin, we examined the localization of fibrillarin in cells treated with hCINAP-specific siRNA. In control cells, fibrillarin predominantly localized in nucleoli and co-localized with coilin in CBs in nucleoplasm (Fig. 3c, white arrows, upper panels), whereas in hCINAP-depleted cells, coilin was distributed in numerous smaller and irregular foci throughout the entire nucleus (Fig. 3c, lower panels), which was consistent with our observations in Fig. 3a (lower panels). Although fibrillarin still predominantly localized in nucleoli in hCINAP-depleted cells, its localization patterns in CBs have changed in nucleoplasm compare to control siRNA-treated cells. The extra-nucleolar foci in which fibrillarin accumulated (Fig. 3c, white arrows, upper panels) were no longer present in hCINAP-depleted cells (Fig. 3c, lower panels).

#### hCINAP deficiency does not cause defects in the expression of coilin, SMN and fibrillarin

Because depletion of hCINAP disrupted the normal localization of coilin, SMN, and fibrillarin in nucleus, we

wanted to know whether hCINAP deficiency will affect the expression of these proteins. As shown in Fig. 3d, knock-down of hCINAP expression in HeLa or HEK 293T cells did not alter the expression levels of coilin, SMN, and fibrillarin, suggesting that hCINAP is required just for the normal subcellular localization of coilin, SMN, fibrillarin, and assembly of CBs.

Redistribution of snRNPs and decreasing of spliceosomal U snRNAs occur in hCINAP-depleted cells

Previous studies suggested that spliceosomal snRNPs do not localize to residual CBs in coilin or SMN-depleted cells [16, 24]. To find out whether depletion of hCINAP affects the subcellular distribution of spliceosomal snRNPs, we examined the localization of spliceosomal snRNPs in hCINAP-depleted cells by staining with antibodies specific to coilin or to the 5'-m<sub>3</sub>G cap of mature U snRNA that is assembled into the spliceosomal snRNP complex. Immunofluorescence analysis demonstrated that the 5'-m<sub>3</sub>G cap U snRNAs localized in CBs (Fig. 4a, white arrows, upper panels) and in speckles in control cells, which are compartments enriched in pre-mRNA splicing factors [40]. While in hCINAP-depleted cells, the 5'-m<sub>3</sub>G cap U snRNAs redistributed from being in both CBs and speckles to be solely in speckles throughout the nucleoplasm (Fig. 4a, lower panels). These observations suggested that hCINAP is required for the normal subcellular distribution of spliceosomal snRNPs and depletion of hCINAP may affect the normal function of spliceosomal snRNPs.

Spliceosomal U snRNPs consist of one or two snRNAs (U1, U2, U4, U5, and U6) and specific sets of proteins. Recent studies indicate that snRNPs transiently localize to CBs for snRNPs maturation, including snRNA base modification and snRNA-protein assembly [7, 41]. Our results shown above indicated that depletion of hCINAP causes defects in the formation of CBs and redistribution of U snRNPs in nucleoplasm. Thus, we examined the levels of U snRNAs in hCINAP-depleted cells by RT-PCR (Fig. 4b). Our results showed that the levels of U1, U2, U4, and U5 snRNAs decreased variously, but no obvious reduction of U6 snRNA observed in hCINAP-depleted cells.

hCINAP co-localizes and associates with NPAT

It has been demonstrated previously that NPAT is concentrated in CBs tethered to histone gene clusters at chromosome 1 and 6 [27]. Moreover, NPAT deficiency leads to dissociation of coilin from CBs and inhibition of histone gene expression [27, 28]. Our results above showed that hCINAP co-localized with coilin in CBs (Fig. 3a, white arrows, upper panels) and that NPAT was detected in

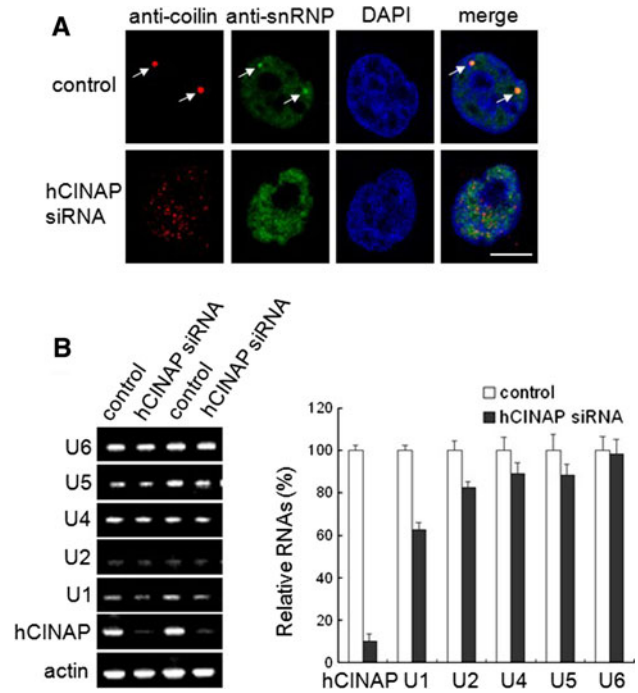


**Fig. 4** Redistribution of snRNPs and decreasing of spliceosomal U snRNAs occur in hCINAP-depleted cells. **a** To determine the localization of snRNPs, HeLa cells that transfected with a control or hCINAP-specific siRNA were subjected to immunofluorescence studies using anti-coilin (red) and anti-m<sub>3</sub>G (green) antibodies. CBs are indicated with white arrows and the nucleus was stained with DAPI (blue). Scale bar 10  $\mu$ m. **b** RT-PCR analysis was performed to examine the hCINAP mRNA and spliceosomal snRNAs levels (left panel). Quantification of hCINAP mRNA and snRNAs was performed using AlphaMager™ software (right panel). The relative amounts (mean  $\pm$  SD,  $n = 3$ ) of hCINAP mRNA and snRNAs normalized to  $\beta$ -actin are presented as a bar graph. A  $p$  value of less than 0.05 was considered to indicate statistical significance

anti-hCINAP immunoprecipitates (Fig. 1b, left panel). Therefore, we examined whether hCINAP is also co-localized with NPAT through immunofluorescent assay. We discovered that hCINAP was overlap with NPAT in punctuate foci (Fig. 5a, white arrows, upper panels). We further identified that hCINAP was co-immunoprecipitated with NPAT (Fig. 5c). In cells that co-transfected with expression plasmids of pCMV-NPAT and pRK-Flag-hCINAP, hCINAP was detected in the anti-NPAT immunoprecipitate but not in the control (Fig. 5c, left panel). Moreover, an endogenous interaction between hCINAP and NPAT was confirmed (Fig. 5c, right panel). These results indicate that hCINAP co-exist with NPAT in a complex and may have an effect on the function of NPAT.

Depletion of hCINAP results in mislocalization of NPAT and inhibition of histone transcription

Our results shown above indicated that hCINAP co-localized and associated with NPAT, and that depletion of

hCINAP by RNAi caused defects in the formation of CBs and relocalization of coilin and SMN in the nucleus. These observations urged us to address the question whether these changes also affected NPAT subnuclear localization and its function on histone transcription activation.

We first verified whether the normal localization of NPAT was disrupted in hCINAP-depleted HeLa cells by laser confocal microscopy. As shown in Fig. 5a (lower panels), knockdown of hCINAP resulted in mislocalization of NPAT, from the normal focal pattern to a diffuse nuclear staining, compare to the control cells (Fig. 5a, upper panels). This observation was further confirmed in Fig. 5b, which showed that depletion of hCINAP caused mislocalization of NPAT from canonical CBs (Fig. 5b, white arrows, upper panels) into a diffuse pattern (Fig. 5b, lower panels). This mislocalization is likely to have functional significance because it is established that NPAT is essential for histone gene expression [29].

Next, we examined histone gene expression in control and hCINAP-depleted cells by RT-PCR assays. Reduction of hCINAP mRNA levels to  $\sim 20\%$  of control had no

obvious effect on the histone gene transcription (data not shown). When the mRNA level of hCINAP was further reduced to  $\sim 5\%$  of control, marked reductions from  $\sim 30$  to  $\sim 60\%$  in the expression of histone genes including H2a, H2b, H3, and H4 were detected (Fig. 5d). These data suggest that hCINAP deficiency results in mislocalization of NPAT and inhibition of histone transcription.

#### Effects of hCINAP deficiency on the cell cycle and cell viability

To further confirm whether the loss of hCINAP also affects cell cycle progression, we analyzed the control and the hCINAP knockdown cells by flow cytometry. Knockdown of hCINAP did not increase the cells in the G0/G1 phase (Fig. 6a). Instead, a decrease of the G0/G1 phase cells and an increase of the sub-G1 phase cells were observed in hCINAP-depleted cells, which indicates higher number of apoptotic cells [42].

Recent studies showed that the homologue of hCINAP in yeast, Fap7, is essential for yeast growth [43, 44]. A

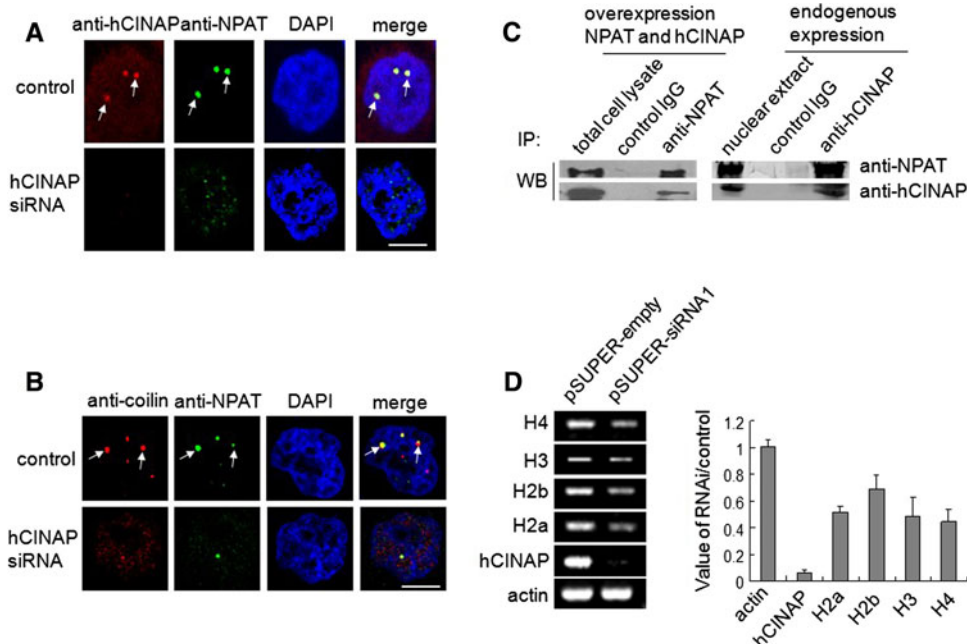


**Fig. 5** hCINAP associates with NPAT and depletion of hCINAP results in mislocalization of NPAT and inhibition of histone transcription. **a** Immunofluorescence studies with antibodies against hCINAP (red) and NPAT (green) were performed in control cells and hCINAP-depleted cells. In control cells, hCINAP and NPAT co-localizes to CBs while these structures become disappeared in hCINAP-depleted cells where NPAT disperses in nucleoplasm. **b** Immunofluorescence assays indicate that depletion of hCINAP disrupts the normal localization of NPAT (green) and coilin (red). CBs are indicated with white arrows and the nucleus was stained with DAPI (blue). Scale bar 10  $\mu\text{m}$ . **c** Association of hCINAP with NPAT. HEK 293T cells were co-transfected with pCMV-NPAT and pRK-Flag-hCINAP. Immunoprecipitation experiment was performed using

an antibody against NPAT, a nonspecific IgG antibody was used as a control (left panel). Endogenous Co-IP was performed to further confirm the interaction between hCINAP and NPAT in HEK 293T cells (right panel). Nuclear extracts were pulled down with either IgG (a negative control) or hCINAP antibody, followed by hCINAP or NPAT immunoblotting. **d** hCINAP depletion inhibits histone transcription. HeLa cells were transfected with pSUPER-hCINAP (siRNA1) or control vector and RT-PCR analysis was performed to examine the mRNA levels of histone genes. Actin amplification was used as loading control. Quantifications of actin, hCINAP, H2a, H2b, H3, and H4 mRNA were performed using AlphaImager<sup>TM</sup> software (mean  $\pm$  SD,  $n = 3$ )

similar result was observed with its homologue in *C. elegans*, ADLP (adrenal gland protein AD-004-like protein), where knockdown of ADLP expression results in the slow growth of worms [33]. Therefore, we examined the effect of hCINAP on cell survival. hCINAP depletion in 293T cells led to about 50% reduction in cell viability when compared to the control cells ( $p < 0.01$ ) (Fig. 6b).

To further elucidate whether the observed loss of cell viability resulted from apoptosis, we examined caspase-3 activity after RNAi treatment. As shown in Fig. 6c, the activity of caspase-3 increased more than twofold in hCINAP RNAi-treated cells. Moreover, the caspase-3 activity was suppressed by Z-VAD-FMK, a caspase-3 inhibitor. These results demonstrate that depletion of hCINAP induces caspase-3 dependent apoptosis. These data demonstrate that hCINAP is essential to cell viability although depletion of hCINAP does not cause an immediate cell cycle arrest.

## Discussion

Recent studies suggest that CBs are composed of diverse components and that they are involved in several nuclear functions [1, 2]; however, the molecular requirement of these components for the formation of canonical CBs is still in part not understood. Here, we identified for the first time that hCINAP protein is associated with some important components of CBs and essential for the formation of CBs by RNAi. Furthermore, we found that hCINAP is required for histone transcription and cell viability.

Our most striking observation is that the normal architecture of CBs and the localization of its components including coilin, SMN, fibrillarin, and NPAT were disrupted upon depletion of hCINAP by RNAi. Recent studies have shown that hCINAP interacts with the C-terminus of coilin, which regulates the number of CBs [19, 32]. Furthermore, overexpression of hCINAP in HeLa cells results

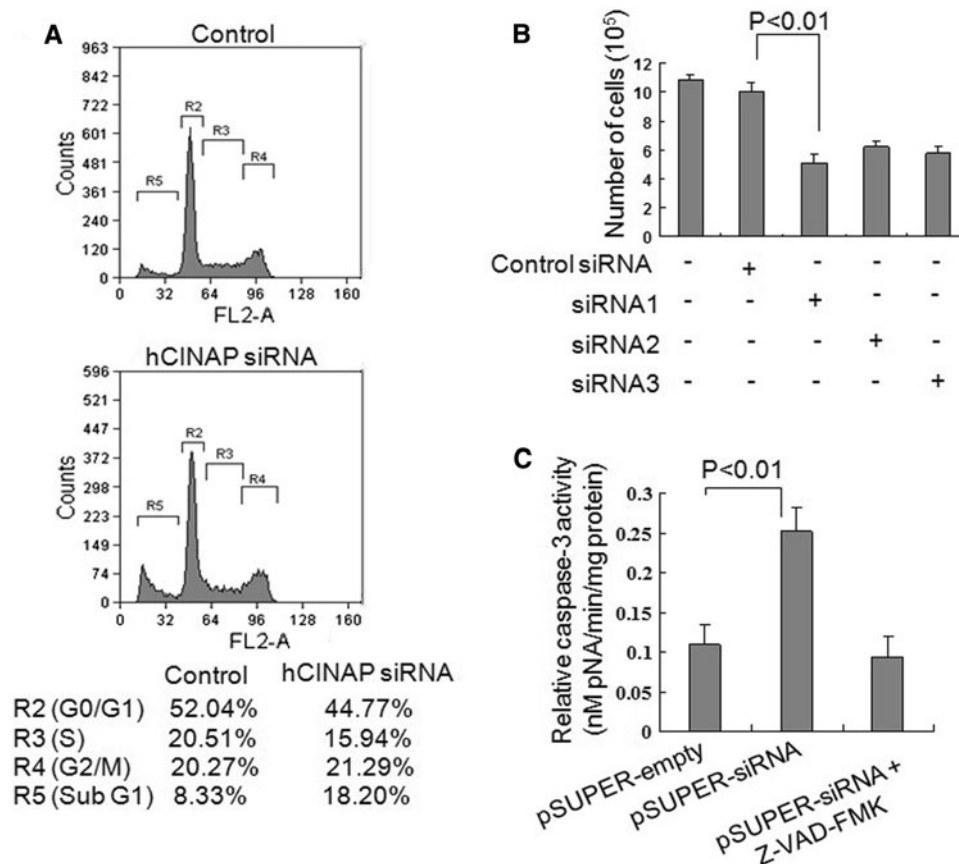


**Fig. 6** Effects of hCINAP depletion on the cell cycle and cell viability. **a** Cell cycle analysis of the HeLa cells transfected with hCINAP siRNA or control siRNA. The histograms show DNA contents of the cells stained with propidium iodide. The percentage of the cells in each cell cycle phase is indicated under each histogram. The sub G1 population represents fragmented nuclei. **b** HEK 293T cells were transfected with indicated siRNAs for 72 h and cell

viability was measured. Data represent the means of five independent experiments, and the bars denote the standard deviation. The  $p$  value ( $p < 0.01$ ) was ascertained by the Student's  $t$  test. **c** HEK 293T cells were transfected with indicated RNAi vector for 72 h and caspase-3 activity was detected in the absence or presence of caspase-3 inhibitor, Z-VAD-FMK. The experiments were repeated three times independently, and  $p$  values ( $p < 0.01$ ) represent the means ( $\pm$ SD)

in a decrease in the average number of CBs per nucleus [32]. We therefore speculated that hCINAP may have a role in modulating either the formation or the stability of CBs. To confirm this speculation, we first examined whether hCINAP co-exists with components of CBs. Our results showed that hCINAP is indeed associated with components of CBs including coilin, SMN, fibrillarin, and NPAT (Fig. 1b). These results suggested that hCINAP is a constituent of CBs. To further investigate the function of hCINAP in CBs, we depleted the expression of hCINAP in HeLa or HEK 293T cells by RNAi. hCINAP depletion resulted in the disappearance of the canonical CBs accompanied by the redistribution of coilin and SMN, the essential components for CBs (Fig. 3a, b). These observations are similar to those caused by deletion of the essential components of CBs such as SMN or FLASH [25, 36].

Previous studies have indicated that SMN plays an essential role in the spliceosomal U snRNP assembly and nuclear import process [24]. After entering the nucleus, snRNPs first target to CBs, where the snRNPs undergo further modification and maturation [7]. Because hCINAP depletion caused defects in the formation of CBs and relocalization of SMN (Fig. 3a, b), we want to know whether hCINAP deficiency may induce changes in the subcellular localization of snRNPs. To test this, we examined the localization of snRNPs in hCINAP-depleted cells using an antibody specific to the 5'-m<sub>3</sub>G cap of U snRNA. Immunofluorescence analysis showed that hCINAP deficiency resulted in relocalization of snRNPs (Fig. 4a). In hCINAP-depleted cells, the 5'-m<sub>3</sub>G cap U snRNAs were distributed solely in speckles throughout the nucleoplasm instead of their localization in both the speckles and CBs in control cells. Examination of snRNAs levels showed that depletion of hCINAP induced decreases of U1, U2, U4, and U5 snRNAs. A recent report indicates that ongoing U snRNP biogenesis is required for the integrity of CBs [25]. Mislocalization of SMN and lower levels of snRNAs in hCINAP-depleted cells probably inhibit the biogenesis of spliceosomal U snRNPs, which may explain why CBs fall apart.

It has been shown that CBs are also involved in the late biogenesis and functional activation of snoRNPs [39]. Since fibrillarin is a core component of mature C/D box snoRNP and is found to co-localize with coilin in CBs, we also examined the localization of fibrillarin in hCINAP-depleted cells, and found that knockdown of hCINAP alters the localization patterns of fibrillarin in extra-nucleolar foci (Fig. 3c).

NPAT is also a component of CBs and it plays an important role in histone gene transcription and cell viability [27, 28]. Our results indicated that hCINAP

co-localized with NPAT in CBs and associated with NPAT (Fig. 5a, c). Moreover, depletion of hCINAP by RNAi disturbed the normal localization of NPAT (Fig. 5a, b, lower panels) and further inhibited the histone genes transcription (Fig. 5d). However, only when the mRNA level of hCINAP was severely reduced to ~5% of control, could the phenomenon of histone transcription inhibition be observed. These results indicate that the amount of hCINAP expression may be taken as a threshold to control the histone transcription. CBs have been shown to associate with histone gene cluster and to regulate histone gene transcription [28, 45]. Hence we think that hCINAP may play an indirect role in regulating histone transcription. Depletion of hCINAP may disrupt the integrity of CBs and normal localization of NPAT, which affects histone transcription. We then examined the effect of hCINAP on cell viability. Consistent with its homologue of Fap7 and ADLP [33, 43], hCINAP depletion resulted in an obvious decrease in the cell viability (Fig. 6b). Although flow cytometry assay showed that hCINAP deficiency did not cause an immediate cell cycle arrest (Fig. 6a), the number of sub-G1 phase cells, which represent apoptotic cells [42], was increased, as was the caspase 3 activity (Fig. 6c). Therefore, apoptosis is one of the reasons responsible for the observed loss of cell viability, although there maybe other mechanisms affecting cell viability after hCINAP siRNA treatment.

Based on the published results and our data, we proposed two possible explanations for the inhibition of formation of CBs. One explanation is that inhibition of the spliceosomal U snRNPs biogenesis causes defects in formation of CBs, as depletion of SMN, hTGS1, PHAX [25], or ZPR1 [37] leads to disappearance of CBs. Another possible interpretation is that deficiency of some important components directly inhibits the formation of CBs. It is reported that coilin, NPAT, and FLASH are the essential components of CBs and that depletion of any of these proteins will disrupt the normal architecture of CBs and result in relocalization of their components [16, 28, 38], which will consequently block snRNPs maturation, U snRNAs and histone transcription or histone pre-mRNA processing [2]. Although we speculate that hCINAP regulates the formation of CBs by inhibition of U snRNPs biogenesis, we cannot completely rule out the possibility that hCINAP itself is important for the integrity of CBs. Therefore, further studies are needed to unravel the precise mechanism of how these proteins, including coilin, NPAT, and FLASH, modulate the formation of CBs.

In conclusion, we have clearly demonstrated that hCINAP is required for the canonical architecture of CBs, histone gene transcription, and cell viability, which help us to further understand the biological functions of hCINAP.

**Acknowledgments** We sincerely thank Dr. Jiyong Zhao for gifting the plasmid of pCMV-NPAT. We thank Dr. Lei Liu for providing equipment used in this study and Xiping Liu for experimental assistance. This work was supported by grants from the National Basic Research Program of China (973 Programs, No. 2010CB911800 and No. 2007CB914303, and 863 Program, No. 2006AA02A314), National Science Foundation of China (No. 30470357), and the International Centre for Genetic Engineering and Biotechnology (ICGEB) (Project No. CRP/CHN09-01).

## References

- Gall JG (2003) The centennial of the Cajal body. *Nat Rev Mol Cell Biol* 4:975–980
- Cioce M, Lamond AI (2005) Cajal bodies: a long history of discovery. *Annu Rev Cell Dev Biol* 21:105–131
- Tomlinson RL, Abreu EB, Ziegler T, Ly H, Counter CM, Terns RM, Terns MP (2008) Telomerase reverse transcriptase is required for the localization of telomerase RNA to cajal bodies and telomeres in human cancer cells. *Mol Biol Cell* 19:3793–3800
- Venteicher AS, Abreu EB, Meng Z, McCann KE, Terns RM, Veenstra TD, Terns MP, Artandi SE (2009) A human telomerase holoenzyme protein required for Cajal body localization and telomere synthesis. *Science* 323:644–648
- Hoareau-Aveilla C, Bonoli M, Caizergues-Ferrer M, Henry Y (2006) hNaf1 is required for accumulation of human box H/ACA snoRNPs, scaRNPs, and telomerase. *RNA* 12:832–840
- Ma X, Yang C, Alexandrov A, Grayhack EJ, Behm-Ansmant I, Yu YT (2005) Pseudouridylation of yeast U2 snRNA is catalyzed by either an RNA-guided or RNA-independent mechanism. *EMBO J* 24:2403–2413
- Darzacq X, Jady BE, Verheggen C, Kiss AM, Bertrand E, Kiss T (2002) Cajal body-specific small nuclear RNAs: a novel class of 2'-O-methylation and pseudouridylation guide RNAs. *EMBO J* 21:2746–2756
- Fu D, Collins K (2006) Human telomerase and Cajal body ribonucleoproteins share a unique specificity of Sm protein association. *Genes Dev* 20:531–536
- Kiss T, Fayet E, Jady BE, Richard P, Weber M (2006) Biogenesis and intranuclear trafficking of human box C/D and H/ACA RNPs. *Cold Spring Harb Symp Quant Biol* 71:407–417
- Matera AG, Shpargel KB (2006) Pumping RNA: nuclear body-building along the RNP pipeline. *Curr Opin Cell Biol* 18:317–324
- Morris GE (2008) The Cajal body. *Biochim Biophys Acta* 1783:2108–2115
- Stanek D, Neugebauer KM (2006) The Cajal body: a meeting place for spliceosomal snRNPs in the nuclear maze. *Chromosoma* 115:343–354
- Kiss T (2004) Biogenesis of small nuclear RNPs. *J Cell Sci* 117:5949–5951
- Ogg SC, Lamond AI (2002) Cajal bodies and coilin—moving towards function. *J Cell Biol* 159:17–21
- Lam YW, Lyon CE, Lamond AI (2002) Large-scale isolation of Cajal bodies from HeLa cells. *Mol Biol Cell* 13:2461–2473
- Tucker KE, Berciano MT, Jacobs EY, LePage DF, Shpargel KB, Rossire JJ, Chan EKL, Lafarga M, Conlon RA, Matera AG (2001) Residual Cajal bodies in coilin knockout mice fail to recruit Sm snRNPs and SMN, the spinal muscular atrophy gene product. *J Cell Biol* 154:293–307
- Hebert MD, Szymczyk PW, Shpargel KB, Matera AG (2001) Coilin forms the bridge between Cajal bodies and SMN, the spinal muscular atrophy protein. *Genes Dev* 15:2720–2729
- Xu H, Pillai RS, Azzouz TN, Shpargel KB, Kambach C, Hebert MD, Schumperli D, Matera AG (2005) The C-terminal domain of coilin interacts with Sm proteins and U snRNPs. *Chromosoma* 114:155–166
- Shpargel KB, Ospina JK, Tucker KE, Matera AG, Hebert MD (2003) Control of Cajal body number is mediated by the coilin C-terminus. *J Cell Sci* 116:303–312
- Frugier T, Nicole S, Cifuentes-Diaz C, Melki J (2002) The molecular bases of spinal muscular atrophy. *Curr Opin Genet Dev* 12:294–298
- Lefebvre S, Bulet P, Liu Q, Bertrand S, Clermont O, Munnich A, Dreyfuss G, Melki J (1997) Correlation between severity and SMN protein level in spinal muscular atrophy. *Nat Genet* 16:265–269
- Pellizzoni L, Yong J, Dreyfuss G (2002) Essential role for the SMN complex in the specificity of snRNP assembly. *Science* 298:1775–1779
- Jady BE, Darzacq X, Tucker KE, Matera AG, Bertrand E, Kiss T (2003) Modification of Sm small nuclear RNAs occurs in the nucleoplasmic Cajal body following import from the cytoplasm. *EMBO J* 22:1878–1888
- Girard C, Neel H, Bertrand E, Bordonne R (2006) Depletion of SMN by RNA interference in HeLa cells induces defects in Cajal body formation. *Nucleic Acids Res* 34:2925–2932
- Lemm I, Girard C, Kuhn AN, Watkins NJ, Schneider M, Bordonne R, Luhrmann R (2006) Ongoing U snRNP biogenesis is required for the integrity of Cajal bodies. *Mol Biol Cell* 17:3221–3231
- Shpargel KB, Matera AG (2005) Gemin proteins are required for efficient assembly of Sm-class ribonucleoproteins. *Proc Natl Acad Sci USA* 102:17372–17377
- Wei Y, Jin J, Harper JW (2003) The cyclin E/Cdk2 substrate and Cajal body component p220(NPAT) activates histone transcription through a novel LisH-like domain. *Mol Cell Biol* 23:3669–3680
- Ye X, Wei Y, Nalepa G, Harper JW (2003) The cyclin E/Cdk2 substrate p220(NPAT) is required for S-phase entry, histone gene expression, and Cajal body maintenance in human somatic cells. *Mol Cell Biol* 23:8586–8600
- Ma T, Van Tine BA, Wei Y, Garrett MD, Nelson D, Adams PD, Wang J, Qin J, Chow LT, Harper JW (2000) Cell cycle-regulated phosphorylation of p220(NPAT) by cyclin E/Cdk2 in Cajal bodies promotes histone gene transcription. *Genes Dev* 14:2298–2313
- Zhao J, Kennedy BK, Lawrence BD, Barbie DA, Matera AG, Fletcher JA, Harlow E (2000) NPAT links cyclin E-Cdk2 to the regulation of replication-dependent histone gene transcription. *Genes Dev* 14:2283–2297
- Ren H, Wang LY, Bennett M, Liang YH, Zheng XF, Lu F, Li LF, Nan J, Luo M, Eriksson S, Zhang CM, Su XD (2005) The crystal structure of human adenylate kinase 6: an adenylate kinase localized to the cell nucleus. *Proc Natl Acad Sci USA* 102:303–308
- Santama N, Ogg SC, Malekkou A, Zographos SE, Weis K, Lamond AI (2005) Characterization of hCINAP, a novel coilin-interacting protein encoded by a transcript from the transcription factor TAF11D32 locus. *J Biol Chem* 280:36429–36441
- Zhai R, Meng G, Zhao Y, Liu B, Zhang G, Zheng X (2006) A novel nuclear-localized protein with special adenylate kinase properties from *Caenorhabditis elegans*. *FEBS Lett* 580:3811–3817
- Brummelkamp TR, Bernards R, Agami R (2002) A system for stable expression of short interfering RNAs in mammalian cells. *Science* 296:550–553
- Zheng X, Dai XY, Zhao YM, Chen Q, Lu F, Yao DQ, Yu Q, Liu XP, Zhang CM, Gu XC, Luo M (2007) Restructuring of the dinucleotide-binding fold in an NADP(H) sensor protein. *Proc Natl Acad Sci USA* 104:8809–8814

36. Barcaroli D, Bongiorno-Borbone L, Terrinoni A, Hofmann TG, Rossi M, Knight RA, Matera AG, Melino G, Laurenzi VD (2006) FLASH is required for histone transcription and S-phase progression. *Proc Natl Acad Sci USA* 103:14808–14812
37. Gangwani L, Flavell RA, Davis RJ (2005) ZPR1 is essential for survival and is required for localization of the survival motor neurons (SMN) protein to Cajal bodies. *Mol Cell Biol* 25:2744–2756
38. Barcaroli D, Dinsdale D, Neale MH, Bongiorno-Borbone L, Ranalli M, Munarriz E, Sayan AE, McWilliam JM, Smith TM, Fava E, Knight RA, Melino G, Laurenzi VD (2006) FLASH is an essential component of Cajal bodies. *Proc Natl Acad Sci USA* 103:14802–14807
39. Matera AG, Terns RM, Terns MP (2007) Non-coding RNAs: lessons from the small nuclear and small nucleolar RNAs. *Nat Rev Mol Cell Biol* 8:209–220
40. O’Keefe RT, Mayeda A, Sadowski CL, Krainer AR, Spector DL (1994) Disruption of pre-mRNA splicing in vivo results in reorganization of splicing factors. *J Cell Biol* 124:249–260
41. Stanek D, Rader SD, Klingauf M, Neugebauer KM (2003) Targeting of U4/U6 small nuclear RNP assembly factor SART3/p110 to Cajal bodies. *J Cell Biol* 160:505–516
42. Ormerod MG (2002) Investigating the relationship between the cell cycle and apoptosis using flow cytometry. *J Immunol Methods* 265:73–80
43. Juhnke H, Charizanis C, Latifi F, Krems B, Entian K-D (2000) The essential protein Fap7 is involved in the oxidative stress response of *Saccharomyces cerevisiae*. *Mol Microbiol* 35:936–948
44. Granneman S, Nandineni MR, Baserga SJ (2005) The putative NTPase Fap7 mediates cytoplasmic 20S pre-rRNA processing through a direct interaction with Rps14. *Mol Cell Biol* 25:10352–10364
45. Gall JG (2001) A role for Cajal bodies in assembly of the nuclear transcription machinery. *FEBS Lett* 498:164–167